



Piraccini, M., Di Maio, D., & Di Sante, R. (2016). Nonlinear modal testing performed by pulsed-air jet excitation system. In G. Kerschen (Ed.), *Nonlinear Dynamics Volume 1: Proceedings of the 34th IMAC, A Conference and Exposition on Structural Dynamics 2016*. (pp. 155-170). (Conference Proceedings of the Society for Experimental Mechanics Series). Springer International Publishing AG. DOI: 10.1007/978-3-319-29739-2_15

Peer reviewed version

Link to published version (if available):
[10.1007/978-3-319-29739-2_15](https://doi.org/10.1007/978-3-319-29739-2_15)

[Link to publication record in Explore Bristol Research](#)
PDF-document

This is the author accepted manuscript (AAM). The final published version (version of record) is available online via Springer at http://link.springer.com/chapter/10.1007/978-3-319-29739-2_15. Please refer to any applicable terms of use of the publisher.

University of Bristol - Explore Bristol Research

General rights

This document is made available in accordance with publisher policies. Please cite only the published version using the reference above. Full terms of use are available:
<http://www.bristol.ac.uk/pure/about/ebr-terms.html>

Nonlinear modal testing performed by pulsed-air jet excitation system

M. Piraccini¹, D. Di Maio², R. Di Sante³

¹ Department of Mechanical Engineering, University of Bristol
University walk, BS8 1TR, Bristol, UK

² Department of Mechanical Engineering, University of Bristol
University walk, BS8 1TR, Bristol, UK

³ Department of Mechanical Engineering, University of Bologna, IT

ABSTRACT

This paper presents a novel approach for testing structural component to nonlinear vibrations. Nowadays, nonlinear testing is mainly carried out by using electromagnetic shakers. These are efficient and powerful excitation systems which transmit the force by a rigid stinger and can be driven by different excitation signals. The rigid connection contributes to create mechanical impedance mismatch between the shaker and the test structure thus reducing the efficiency of the driving force. An alternative solution to shakers is represented by use of a pulsed air jet excitation method, which drives the force by a pulsed air-jets and therefore contactless. This condition eliminates the mechanical impedance mismatch with the test structure and the excitation can be more efficient than the one created by shakers. The pulsed air-jet excitation system is used to study nonlinear vibrations of composites components. These were designed to be mock-ups of fan blades the layup of which was varied for the three types of components used in this work. Tests were carried out by performing forced response and free decay measurements. The free decay type of test revealed interesting results and the novelty of using such an exciter for nonlinear testing. The major novelty consists of interrupting the air flow from a steady state condition and let happen the free decay, all these without experiencing undesired dynamics as experienced by contact excitation.

KEYWORDS: Pulsed air-jet exciter, nonlinear vibrations, composites

1 INTRODUCTION

In recent years, there has been an increasing interest in studying the behaviour of structures presenting nonlinearities [1]. This is primarily due to the increased use of new materials such as composites. For example, over 50% of the structural components of the Boeing 787 and Airbus 350 XWB are made of composite materials [2], which are inherently more flexible and less damped, being therefore more prone to nonlinear behaviour. Hence, the understanding of their performance under

operating conditions, especially when extreme loads are present, has become increasingly important. Different methodologies have been used to get a deeper insight into the dynamics of nonlinear systems [3]. This paper focuses in particular on the nonlinear resonant method (NL-RDM) and on the experimental testing apparatus and procedure supporting this identification method. The NL-RDM was firstly presented in 2001 [4] and refined in subsequent works [5, 6]. The method uses responses obtained from burst or narrowband excitation of the structure at the natural frequency of the mode of interest. When the excitation ends, the responses are allowed to decay freely. Only the concerned mode and the modes nonlinearly coupled to it contribute to the response, allowing the nonlinear identification of the mode itself. Such an approach proves effective to analyse structures that are linear at low vibration amplitudes, but show increasingly larger active elements of nonlinearity at higher excitation levels. This is the case of many industrial structures. The nonlinear resonant method has been applied experimentally to different structures. In [5] Platten et al. characterised successfully the first three modes of a clamped panel structure, in which they had introduced a distributed nonlinearity by stretching the panel's middle surface. In [6] the same authors identified the first five modes of an aircraft like wing/store/pylon structure with discrete hardening stiffness nonlinearity introduced in the pylon. In these works, electrodynamic shakers were rigidly connected to the test structures to provide the burst excitation required by the method. More recently, Londono et al [7] applied a modified version of the method to a single-degree-of-freedom system represented by a base-excited mass mounted on bearings sliding with low friction along steel shafts. The mass was also connected to two preloaded transversal springs which produced nonlinear stiffness. In all these cases, contact excitation provided by shakers is employed to drive each mode separately. This can be an issue [5] since the force is not in phase with the driving voltage and tuning is affected by the severe shaker-structure interaction. Consequently, second harmonics appear in the force signal. Furthermore, when the excitation ends, the stinger is still attached to the structure thus possibly affecting its dynamic behaviour. In order to overcome the problems related to the interaction between the test structure and the excitation device, in this paper a different contactless excitation method is proposed. Compressed air is used to generate a flow which is then chopped by a spinning disc with a series of holes drilled in it. The excitation frequency is therefore given by the number of holes and the rotation speed. After the sudden interruption of the airflow, the responses are allowed to decay freely and without constraint to the excitation system. The paper is organised as follows. Section 2 describes the pulsed-air excitation system proposed in this work. Section 3 reports the design and realisation of the composite blades used in the experiments. Forced and free-decay responses obtained during the tests are presented in Section 4 together with a description of the procedure used for signal processing.

2 PULSED AIR JET EXCITATION SYSTEM

This section will present a contactless excitation system which works by using compressed air. Figure 1 shows the schematic of the excitation system. It is rather simple mechanism based on compressed air flowing into a plenum chamber throughout an orifice. A spinning disc, designed with several holes, opens and closes the orifice thus generating air-jets. The dynamic range of the exciter is given by the capacity of electric motor (max velocity) and by the number of holes on the disc. The actual excitation frequency is given by the following equation:

$$\omega_n = \frac{\Omega}{60} n_{DH}$$

where, ω_n is the excitation frequency, Ω rotational speed of the disc and n_{DH} the number of holes designed for the disc.

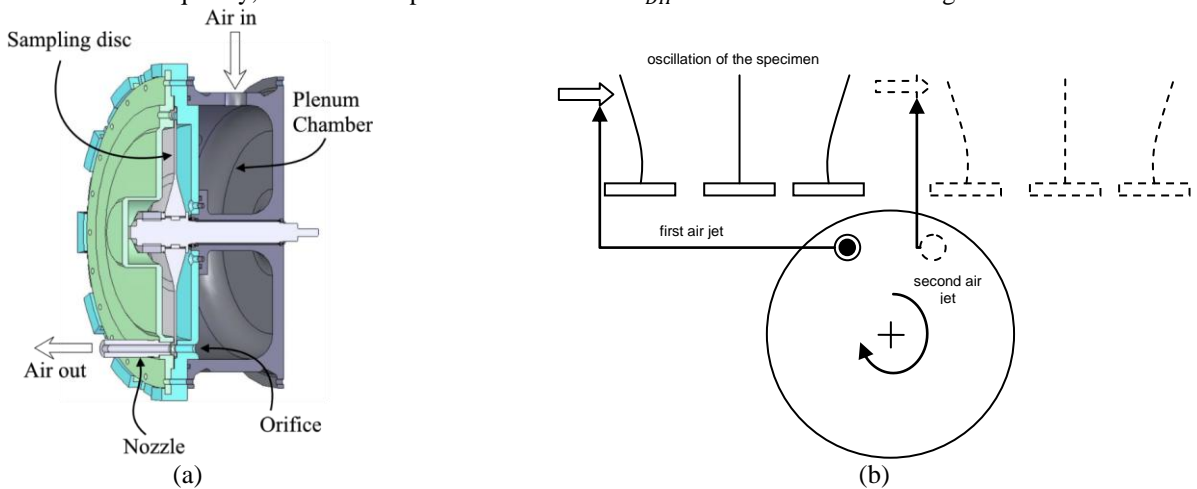


Figure 1 (a) Mechanical scheme of pulsed air-jet system and (b) the operating principle

Several measurements to experimentally quantify the influence of some design parameters were carried out. For example, the ducting (comprising of orifice, sampling hole and nozzle) or the addition of a double nozzle were presented in [8]. To characterize the excitation force with respect of the measured pressure at the nozzle and the excitation frequency, a small test rig was configured as shown in Figure 2. The nozzle was once addressed over the pressure gauge and once over the load cell. The test was repeated at different excitation frequencies. The results are plotted in Figure 3.

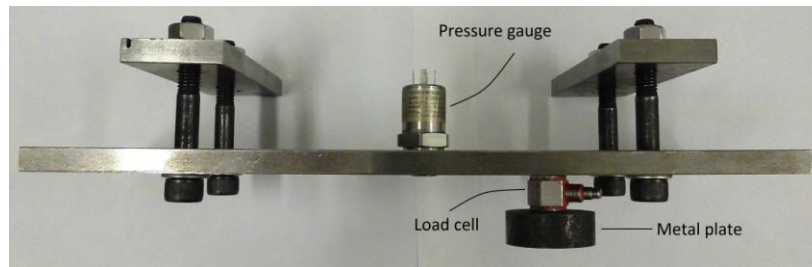


Figure 2 test rig for force vs. pressure characterization

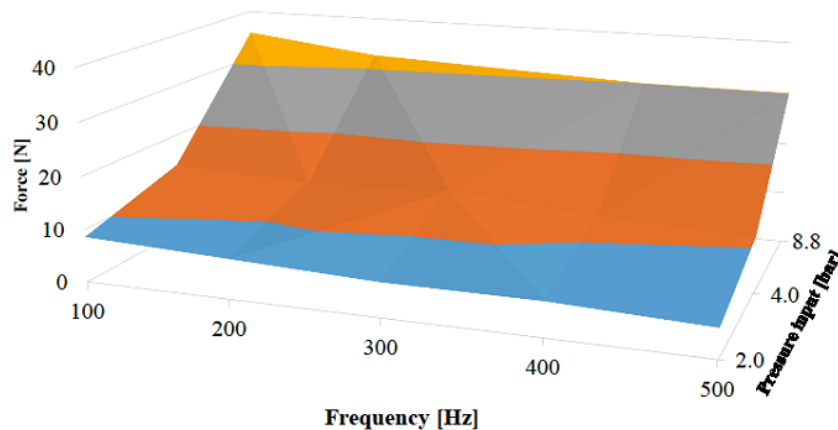


Figure 3 Relationship between excitation force, pressure and excitation frequency

The excitation system, as presented in here, has got some useful features but also some disadvantages. In fact, the pulsed excitation generates harmonics at multiple of the fundamental one. This can determine some undesired effects like parasitic excitation, where some vibration contents can be summed to the one excited by the fundamental tone. However, this is expected and can be monitored accordingly.

The goodness is in its contactless feature which can make the system very convenient when a ramp-down test is aimed. The exciter can generate a steady-state vibration and that is sustained as long as the compressed air flows throughout the system. A free decay can be therefore obtained by abruptly interrupting the airflow, thus letting the vibration of the component to decay. This approach was used to characterize the nonlinear response of cantilever composite blades. The free decay is inherently a challenging type of testing because the excitation source cannot be disconnected so easily from the test structure. If the exciter, such as a shaker, is left connected then its dynamics can influence the results. This is more plausible when high amplitude levels are aimed for.

3 DESIGN AND MANUFACTURING OF THE COMPOSITE BLADES

In this section an outline of the considerations, analyses, constraints, and decisions made about how to design the composite blades object of this work is presented. Manual envelope bagging technique is explained as applied to the actual manufacturing of the components. Difficulties encountered in manufacturing the blades are explained and the methods used to solve them are detailed.

3.1 Design considerations

The objective was to excite geometrically nonlinear vibration and so one side of the blade was thought to be straight, whereas the other one was designed so as to create an angle of $90^\circ + \beta$ between the edge and the base. Different twisting angles θ , thicknesses s , and blade length L were examined in finite element analyses. The following values of the aforementioned parameters were all modelled, see Table 1.

Parameters	Value-1	Value-2	Value-3
Trapezoidal angle (β)	5°	10°	15°
Twisting angle (θ)	10°	20°	---
Thickness (s)	2mm	3mm	---
Length (L)	100mm	300mm	500mm

Table 1 Design parameters

The mode shapes of interest in the analyses were the 1st flexural, the 1st torsional, and the 2nd flexural. From finite element analyses it was possible to notice that a blade long 100mm would be too stiff and have too high natural frequencies as the frequency range of interest was up to 400-500 Hz because of the difficulties to properly excite the vibration and measure it with higher natural frequencies. Moreover some combinations of parameters led to natural frequencies that were too close one another; it would be then difficult to analyse the dynamics of such a structure as it would not be allowed to use the 1DOF approximation. Since it was subsequently known the composite roll was 300mm in width it was evident that a blade long 500mm would not optimise the nesting during the cutting of the composite plies. A flat area long 54mm was thought to be adequate to properly clamp the blade during vibration tests. The length of 280mm optimised the cutting process by reducing the waste during cutting. Thus, either to reduce the composite waste or to have natural frequencies of the first three mode shapes in the range of interest, the possible length had to be close to 300mm. A 10°-twisting-angle was deemed too small to be practically realised and the 20° value for the twisting angle was chosen. The trapezoidal angle was chosen to be 5° as it seemed to lead to better mode shapes. Since the blade had to contain 4 ply drops, with a consequently change in thickness of 0.5mm (being each ply 0.125-thick), a 3mm-thickness was more adequate to experience such a change; moreover the flat rectangular specimens with ply drops previously tested during another research project were 3mm-thick and the thickness change created no problems so that it was thought to be expedient to use such a previous validation. Final choices for the parameters of the blade can be seen Figure 4.

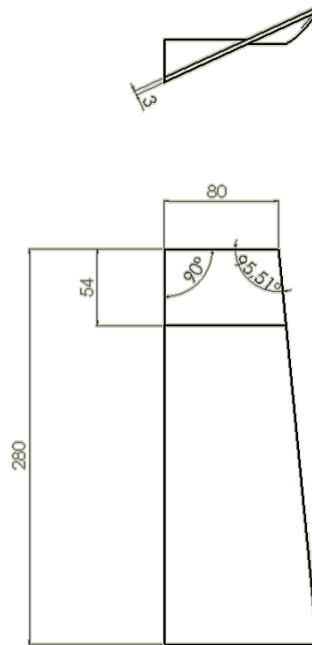


Figure 4 Definitive dimensions for the composite blade

Three different layups were made so as to test the different dynamics with varying fibre directions. Since subsequent fatigue tests would be carried out by exciting the specimens at the 2nd flexural mode, the ply drops were not located on the surface of the blade as the bending normal stress is maximum in that area, but two full plies were allowed to be present in the zone of maximum stress. Since each ply has an after-cured-thickness of 0.125mm, 24 plies were used for the three specimens. The chosen stacking sequences were symmetric across their mid-plane in order to exhibit no coupling between bending and extensional responses; one important practical implication is that such laminates do not have a tendency to bend or twist from the inevitable thermally induced contractions that occur during cooling following the curing process. The fibre orientations were unidirectional 0°, cross-ply [0/90]s and balanced angle-ply [+45/-45]s. Cross-ply laminates exhibit no coupling either

between shear and extensional response and between bending and twisting response. A symmetric angle-ply laminates does not have shear-extensional coupling effects.

After making the first blade a problem became evident; the area designed to be flat so as to be properly clamped during vibration tests was not sufficiently flat. In fact, the bottom surface, which was in contact with the mould, appeared completely flat whereas the top surface experienced a slight curvature that impeded a correct clamp of the blade. Thus, the first blade manufactured was not deemed adequate to be experimentally tested. In a second attempt the aforementioned problem was solved by means of a top plate that was cut and applied on the composite during the curing cycle in order for the blade to have both surfaces under compression. In this way, a uniform pressure could be exerted on the root of the blade during the autoclave cycle and both bottom and top surfaces were perfectly flat.

4 EXPERIMENTAL WORK

In order to carry out forced response analyses it was decided to use only contactless methods for both the excitation and the measurement systems. The test rig was made as shown in the Figure 5 where the exciter is positioned at the top left corner of the specimen. This way all 3 modes could be excited. As can be seen from Figure 5, the blade was clamped to a specific base designed in order to provide very accurate clamp, hence reducing the possibilities of the presence of contact nonlinearities and energy dissipation in the clamp. A guillotine was placed in front of the airflow in order to cut the air in following decay analyses. A nozzle was used to bring the flow as close as possible to the excitation point so as to create as much a homogeneous fluid dynamics as possible. The vibration velocity was measured by means of a Polytec PSV400 Laser Doppler Vibrometer with sensitivity of 2m/s/V in the single-point mode of use.



Figure 5 Text fixture, blade and exciter's nozzle

The scanning head was set outside the anechoic chamber containing the blade and exciter. Since detection of superharmonics in nonlinear vibration was one of the goals of the subsequent decay analyses, a low pass filter was set at a high frequency (20 kHz) to allow the investigation of a wide range of frequency content in the signal.

In order to increase the reflection from the surface of the blade, reflective tape was used at the point of measurement. The forced response was acquired by using a LabVIEW programme and the frequency of excitation was set by using a control panel for regulating the speed of the electric motor of the exciter. By regulating the airflow by means of opening or closing the flow control valve of the chopped air machine, different excitation intensities were adopted in order to characterise the behaviour of the 1st flexural, 1st torsional, and 2nd flexural mode shapes of the three different layups at increasing displacements. After localising the resonant frequencies, tests were carried out on each of the first three mode shapes by exciting each blade in a frequency range around its natural frequencies and repeating the tests at different levels of excitation (i.e. different airflow intensities).

4.1 Experimental results

The following graphs summarise the global measured forced responses and give the natural frequency change with regard to the measured amplitude of the displacement.

4.1.1 Unidirectional: 1st flexural mode

The 1st flexural vibration of the unidirectional 0°-angled blade has been studied by means of exciting the component around its linear natural frequency (74 Hz) with six increasing airflow intensities. From forced responses (Figure 6 (a)) it can be seen that even with the lowest excitation intensities the amplitude of the vibration of the unidirectional blade at the first mode shape was extremely high. The behaviour of the blade vibrating with the 1st flexural mode shape is evidently linear as there is no significant frequency variation with varying amplitude even if the displacement becomes very large as can be seen from backbone curve in Figure 6(b).

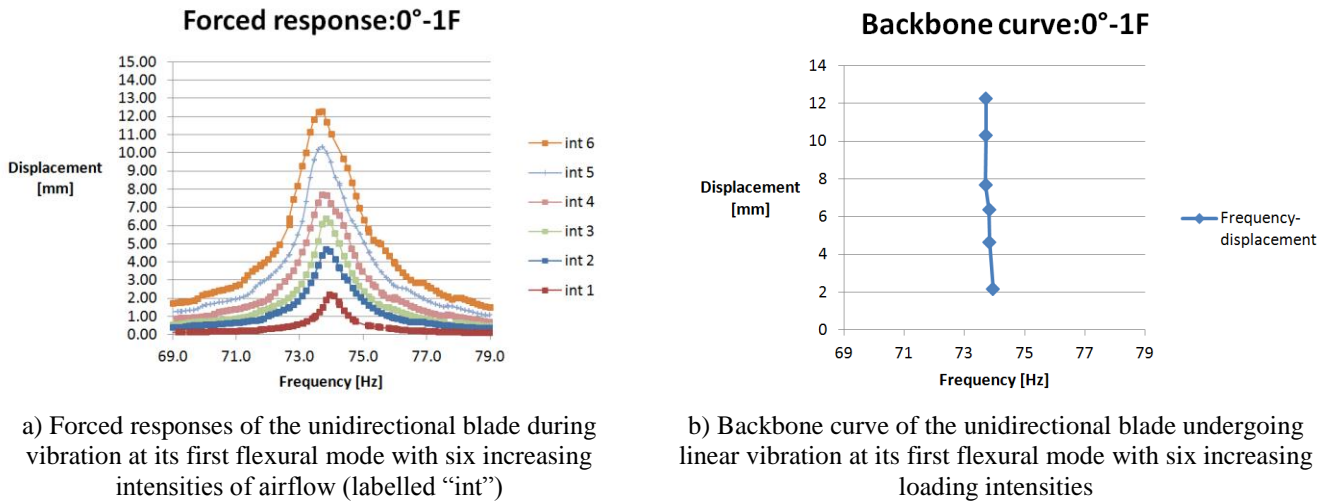
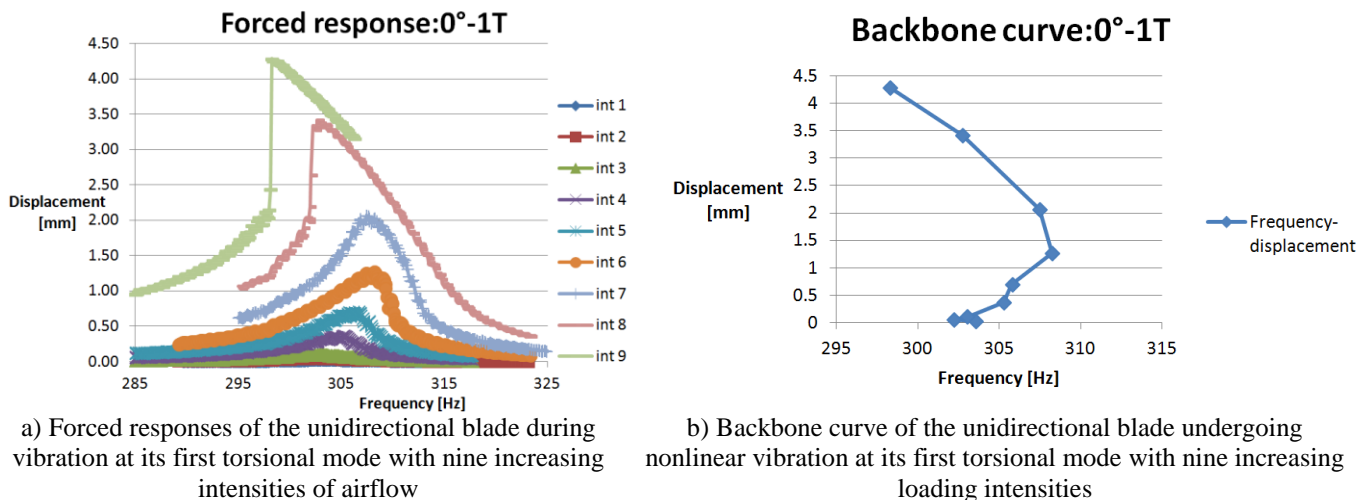


Figure 6 First bending mode

4.1.2 2.3.2- Unidirectional: 1st torsional mode

The vibration of the 1st torsional mode of the 0° blade is extremely singular and markedly nonlinear. Nine increasing airflow intensities were investigated so as to be able to fully characterise such a varying behaviour. From Figure 7(a) it can be seen that jump phenomena start to appear when the peak of the vibration approaches the value of the thickness of the blade (i.e. 3mm) and the vibration abruptly changes its intensity. This is coherent with the known consideration that significant nonlinearities most often appear when displacement is comparable to the thickness. From Figure 7(b), which represents the backbone curve of the vibration, it can be noted that vibration changes its behaviour as displacement approaches 1.5 mm from a hardening nonlinear type of vibration to a softening nonlinearity underlining a change in the laminate stiffness.

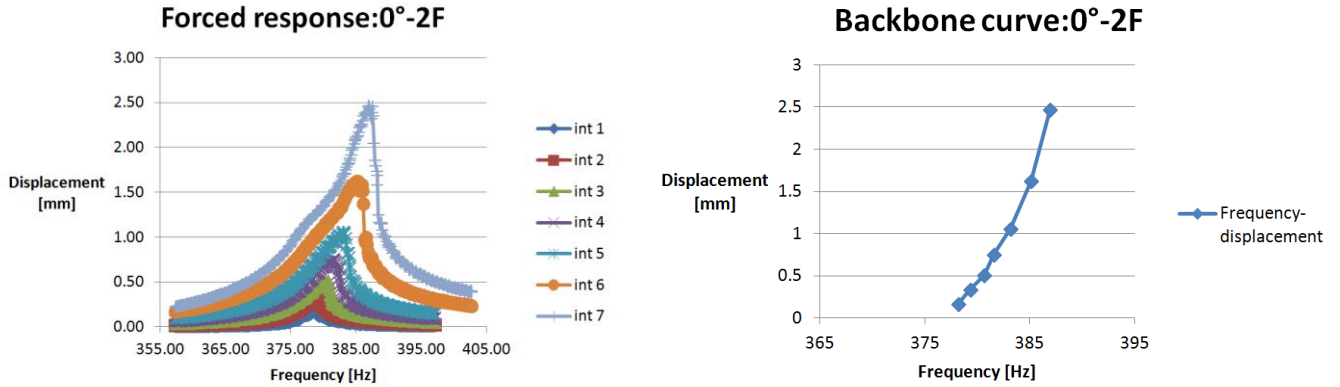


b) Backbone curve of the unidirectional blade undergoing nonlinear vibration at its first torsional mode with nine increasing loading intensities

Figure 7 First torsional mode

4.1.3 *Unidirectional: 2nd flexural mode*

Differently from the first flexural mode the 2nd flexural mode exhibits a strong hardening behaviour; in Figure 8(a) jump phenomena are also evident starting at around 1.5 mm. Backbone curve in Figure 8(b) shows natural frequency increasing with increasing vibration amplitude.



a) Forced responses of the unidirectional blade during vibration at its second flexural mode with seven increasing intensities of airflow

b) Backbone curve of the unidirectional blade undergoing nonlinear vibration at its second flexural mode with seven increasing loading intensities

Figure 8 Second bending mode

4.2 *Free decay procedure and signal processing*

The following experimental procedure was used in order to characterise the behaviour of free decay responses. By using the same experimental equipment as those used for the forced response tests, the airflow was cut by using a guillotine and the vibration was acquired via LDV system during free decay. The so-acquired velocity signal was integrated to give the displacement and then analysed by using a spectrogram, also called sliding Discrete Fourier Transform, meaning that the frequency content was derived by using Fast Fourier Transform algorithm applied to a sliding window over time. Thus, it is possible to visualise either the frequency content and how different frequencies appear and disappear in the signal during the decay. Discrete Fourier Transform over the entire decay time was also applied to have an idea of how strong each frequency component in the signal was. After isolating the fundamental frequency of vibration by means of a second-order band-pass filter to adopt a one-degree-of-freedom model, the logarithmic decrement of the decay was computed and the damping ratio associated with the excited mode shape was analysed as a function of amplitude for those modes which had a viscous-like damping. The entire procedure was made up of the following steps and repeated at different levels of excitation.

Acquiring the decay signal of the velocity from Polytec LDV system as shown in Figure 9.

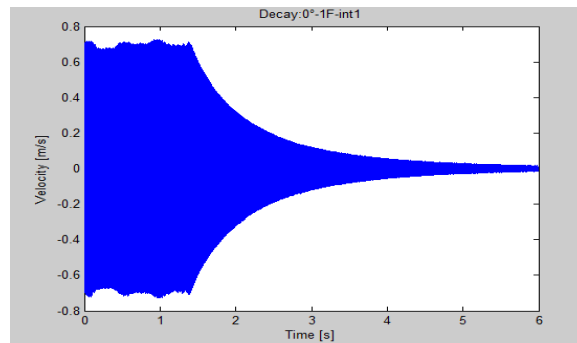


Figure 9 Acquisition of the velocity decay from Laser Doppler Vibrometer

Integration of the velocity in order to obtain the displacement signal. Computing the spectrogram (i.e. sliding Discrete Fourier Transform with Hamming windowing) of the signal to visualise the frequency content present during the decay, see Figure 10. Computing DFT over the entire signal to visualise the strength of each frequency component in the signal, see

Figure 11.

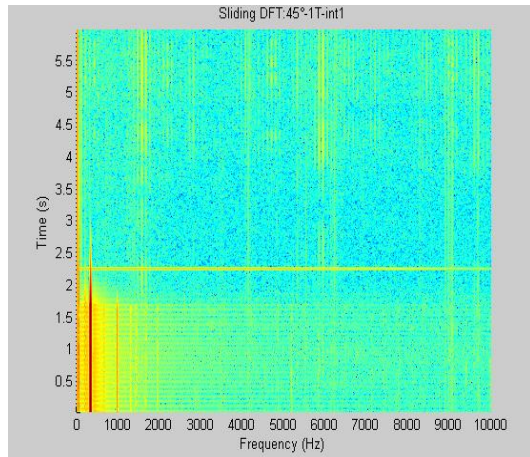


Figure 10 Sliding DFT computation with Hamming windowing

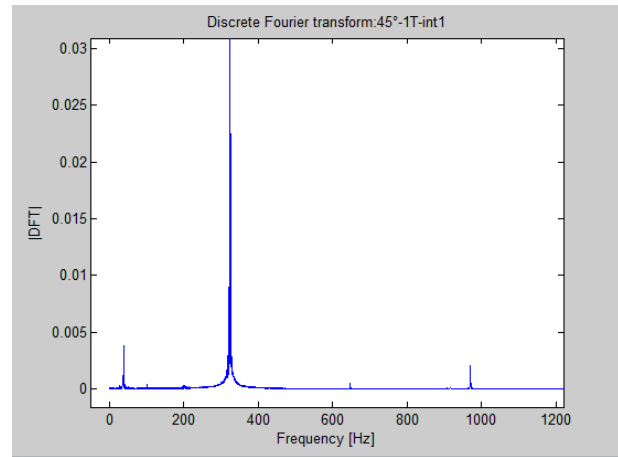


Figure 11 Computation of the Discrete Fourier Transform of the acquired signal to visualise how strong frequency component are

Applying a band-pass filter to isolate the fundamental frequency associated with the externally excited mode shape, see Figure 12.

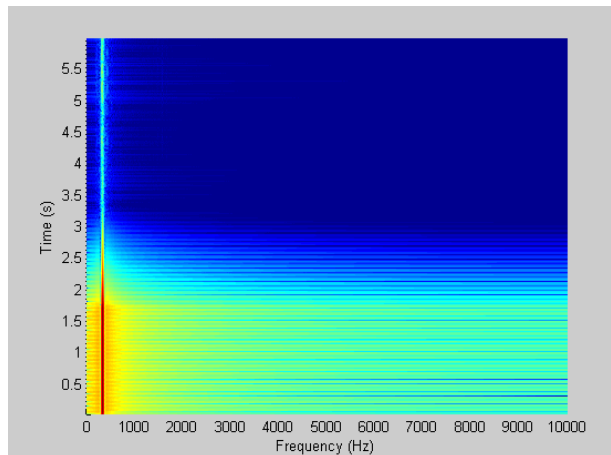


Figure 12 Application of band-pass filter to isolate the fundamental resonant frequency associated with the excited mode

Dividing the filtered signal in its positive and negative branches and envelope detection by means of peak recognition, see Figure 13.

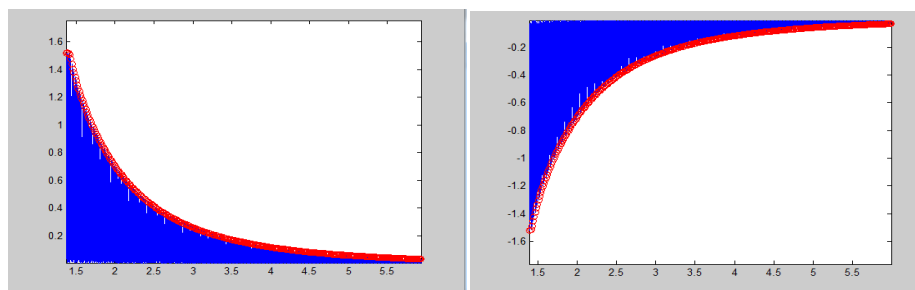


Figure 13 The signal is divided in its positive and negative part in order to compute both the decay rates by means of peaks detection

Computation of the logarithmic decrement and subsequently the damping ratio as shown in Figure 14.

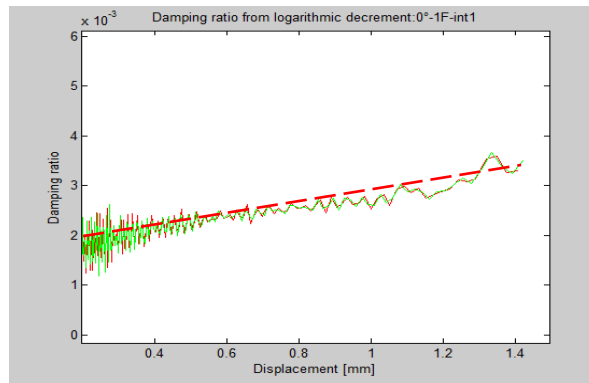


Figure 14 Damping ratio computation as a function of the amplitude of vibration

The proposed procedure was applied to different excitation levels. The following section will present some results obtained by using this procedure.

4.3 Free decay experimental results

4.3.1 Unidirectional: 1st flexural mode

Figure 15, Figure 16 and Figure 17 show the time decay signal for three different excitation forces. The 1st flexural mode associated with the unidirectional blade is confirmed to be strongly linear as no superharmonics appear in the frequency spectrum (Figure 18) and damping phenomenon is uniquely viscous-like damping (i.e. exponential decay). The logarithmic decrement and subsequent damping ratio underline a tendency to an increase in the damping values with increasing amplitude level (Figure 19).

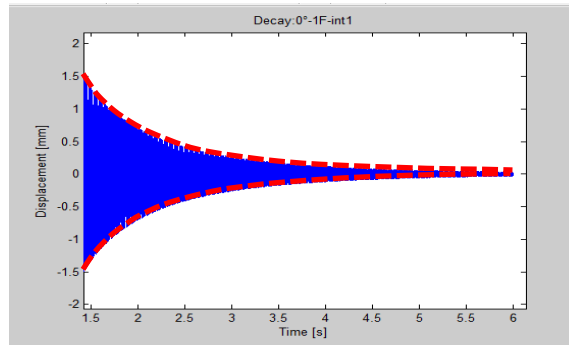


Figure 15 Displacement decay of the unidirectional blade vibrating at first flexural mode. Decay intensity 1.

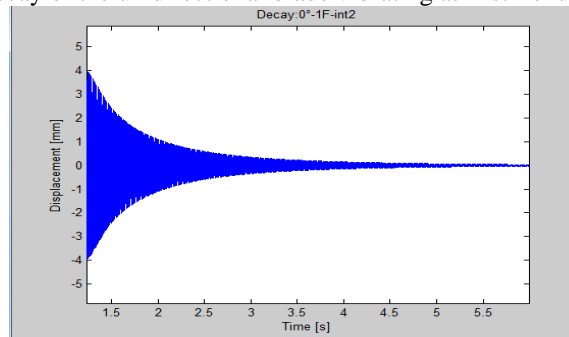


Figure 16 Displacement decay of the unidirectional blade vibrating at first flexural mode. Decay intensity 2.

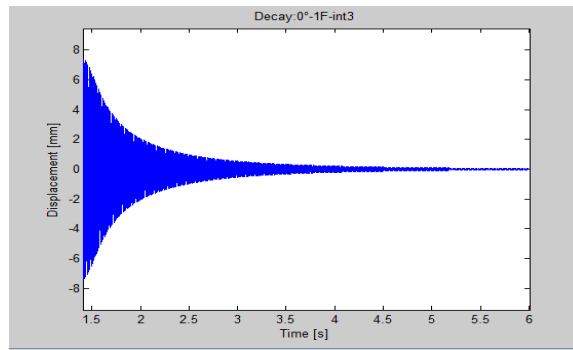


Figure 17 Displacement decay of the unidirectional blade vibrating at first flexural mode. Decay intensity 3.

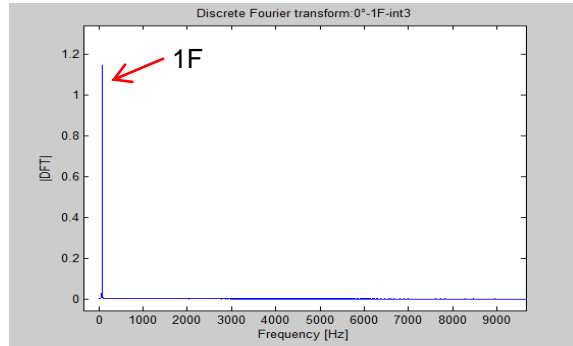


Figure 18 Frequency spectrum shows no nonlinearities. Decay intensity 3.

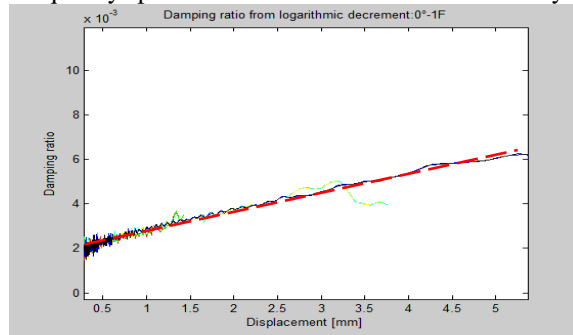


Figure 19 Damping ratio linearly increases with increasing vibration amplitude

4.3.2 Unidirectional: 1st torsional mode

The first torsional mode associated with the unidirectional blade is confirmed to be strongly nonlinear by the presence of at least four superharmonics in the decay signal at the highest intensity, as shown in Figure 20. The intense presence of the frequency associated with the first flexural mode in the frequency spectrum of the signal (Figure 21) may indicate a 1:4 internal resonance phenomenon between the torsional (305Hz) and flexural (74Hz) modes in which energy is transferred by means of a nonlinear coupling from external resonance of the torsional motion to internal resonance of the flexural motion. From Figure 22 it can be seen that as the time elapses and vibration amplitude is successively damped out causing the displacement to decrease over time, only the first flexural resonance appears. This indicates that even if the forcing frequency from which the decay starts was set at the torsional resonance, at small displacements energy is transferred to lower mode shapes.

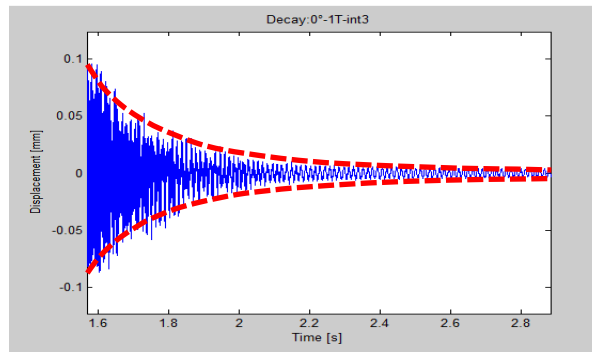


Figure 20 Velocity decay of the unidirectional blade vibrating at first flexural mode. Decay intensity 4

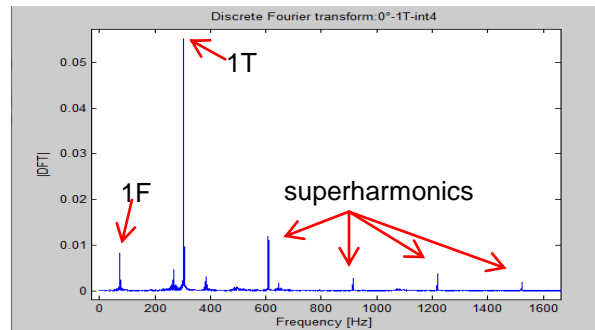


Figure 21 Frequency spectrum shows four superharmonics of the torsional fundamental frequency and an intense presence of the first flexural natural frequency. Decay intensity 4

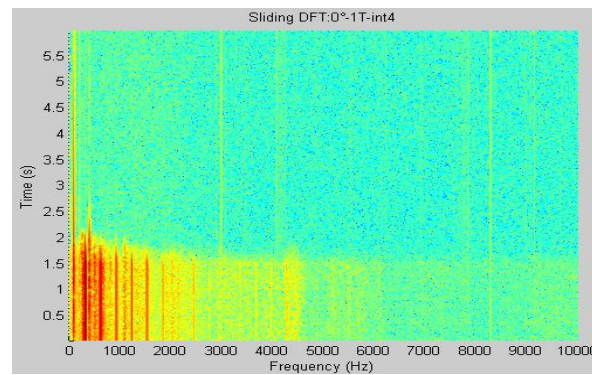


Figure 22 Sliding frequency spectrum over time clearly shows vibration damps out the superharmonics during the decay as time elapses and vibration amplitude decrease. Decay intensity 4

4.3.3 Unidirectional: 2nd flexural mode

The 2nd flexural mode of the 0° blade is confirmed highly nonlinear by the presence of four superharmonics in the signal at the highest excitation intensities (Figure 25 and Figure 26). Interestingly, the damping phenomenon changes from viscous damping at small amplitude vibration (Figure 23) to Coulomb-like damping at high displacement (Figure 24) introducing further nonlinear behaviour.

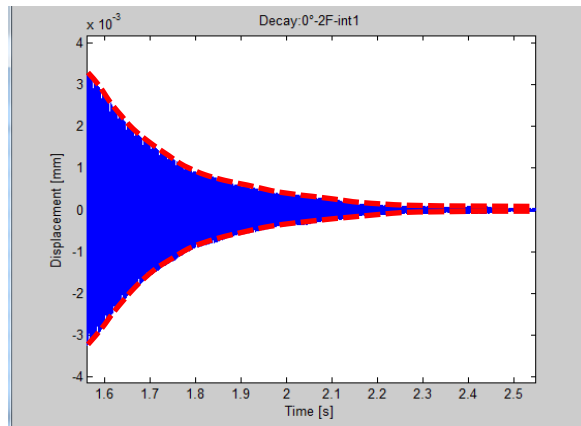


Figure 23 Displacement decay of the unidirectional blade vibrating at second flexural mode with small amplitude. Damping can be approximated by a viscous model. Decay intensity 1

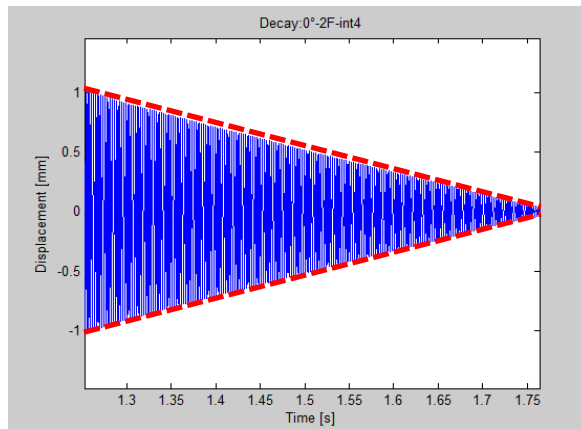


Figure 24 Displacement decay of the unidirectional blade vibrating at second flexural mode with large amplitude. Damping can be approximated by a dry friction model. Decay intensity 4

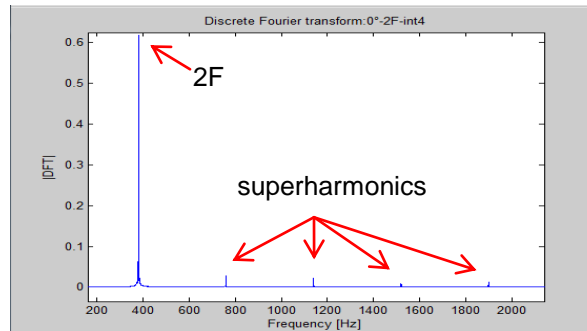


Figure 25 Frequency spectrum shows four superharmonics of the second flexural fundamental frequency. Decay intensity 4

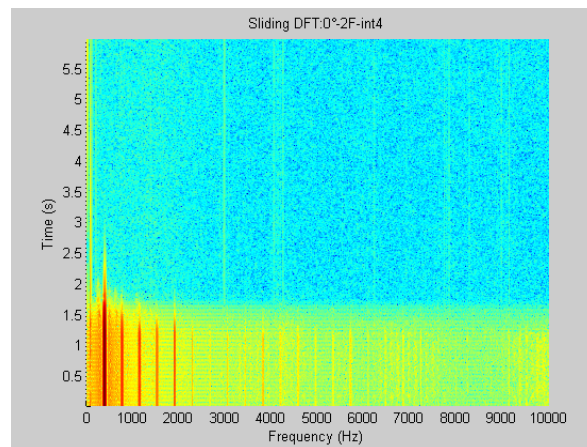


Figure 26 Sliding frequency spectrum over time clearly shows vibration damps out the four superharmonics during the decay as time elapses and vibration amplitude decreases. A wide frequency range is present in the signal indicating extremely strong nonlinear behaviour. Decay intensity 4

5 CONCLUSIONS

The pulsed air-jet excitation system is used in this work for inducing high vibration amplitudes of composites components. Despite this system was designed for High Cycle Fatigue testing thanks to its contactless feature, it was understood that such a feature could be well exploited for nonlinear testing. The major advantage is to allow steady state conditions at any excitation frequency and from which a free decay can be initiated. The same system can be also used for forced response testing. Some staggered composite blades were manufactured and tested in both free-free decay and forced response measurements. The blades were manufactured by creating three different layouts and results of experiments were presented in here. Few drawbacks can be pinpointed and these are the excitation type which is pulsed and not harmonic. This can determine additional excitation components to the fundamental one. The other pitfalls could be seen in the air-jet which is only push and therefore this system would not be suitable for testing under free-free conditions. Nevertheless, the authors believe that the dynamic community should be informed of such an excitation so as to encourage further developments.

REFERENCES

- [1] K. Worden, G. Tomlinson, *Nonlinearity in Structural Dynamics: Detection, Identification and Modelling*, IOP Publishing Ltd, Bristol, Philadelphia, 2001.
- [2] Di Sante, R. *Fibre Optic Sensors for Structural Health Monitoring of Aircraft Composite Structures: Recent Advances and Applications*. *Sensors* 2015, 15, 18666-18713.
- [3] A. Carri, D. Ewins, A systematic approach to modal testing of nonlinear structures, R. Allemang, J. De Clerck, C. Niezrecki, A. Wicks (Eds.), *Topics in Modal Analysis Conference Proceedings of the Society for Experimental Mechanics Series, Vol. 7, Springer, New York 2014*, pp. 273–286.
- [4] Wright, J. R., Platten, M. F., Cooper, J. E., and Sarmast, M., *Identification of Multi Degree of Freedom Weakly Nonlinear Systems Using a Model Based in Modal Space*, *Proceedings of the COST International Conference on Structural System Identification*, Universitätsbibliothek Kassel, Kassel, Germany, 2001, pp. 49–68.
- [5] Platten, M. F., Wright, J. R., Dimitriadis, G., and Cooper, J. E., *Identification of Multidegree of Freedom Nonlinear Systems Using an Extended Modal Space Model*, *Mechanical Systems and Signal Processing*, Vol. 23, No. 1, 2009, pp. 8–29.
- [6] Platten, M. F., Wright, J. R., Cooper, J. E., and Dimitriadis, G., *Identification of a nonlinear wing structure using an extended modal model*, *Journal of aircraft*, Vol. 46, No. 5, 2009, pp. 1614-1626.
- [7] Londono, J. M., Neild, S. A., and Cooper J. E., *Identification of backbone curves of nonlinear systems from resonance decay responses*, *Journal of Sound and Vibration*, 348, 2015, pp. 224-238.
- [8] Di Maio, Dario, and Fabrizio Magi. *Development of testing methods for endurance trials of composites components*. *Journal of Composite Materials*, 2015, vol. 49, no. 24, 2977-2991.